

# Evidence for exhaustion in the conductivity of the infinite-dimensional periodic Anderson model

A. N. Tahvildar-Zadeh and M. Jarrell

*Department of Physics, University of Cincinnati, Cincinnati, Ohio 45221*

Th. Pruschke

*Institut für Theoretische Physik, Universität Regensburg, Regensburg, Germany*

J. K. Freericks

*Department of Physics, Georgetown University, Washington, D.C. 20057*

(Received 10 June 1999)

Monte Carlo–maximum entropy calculations of the conductivity of the infinite-dimensional periodic Anderson model are presented. We show that the optical conductivity displays anomalies associated with the exhaustion of conduction-band states near the Fermi energy including a Drude weight, which rises with temperature, with weight transferred from a temperature and doping-dependent mid-infrared (IR) peak and a low-frequency incoherent contribution. Both the Drude and mid-IR peaks persist up to very high temperatures. The resistivity displays a nonuniversal peak and two other regions associated with impuritylike physics at high temperatures and Fermi-liquid formation at low  $T$ . [S0163-1829(99)04839-0]

## I. INTRODUCTION

Metallic compounds containing rare earth elements with partially filled  $f$  shells, such as CeBe<sub>13</sub> or UPt<sub>3</sub>, belong to the general category of heavy fermions materials.<sup>1</sup> They are characterized by a large Pauli susceptibility and specific heat as compared to ordinary metals, which indicate a large effective electronic mass, and also by anomalous transport properties such as nonmonotonic temperature dependence of the resistivity. These anomalies are usually attributed to the formation of a resonant state at the Fermi energy, associated with moment screening, due to the admixture of the electronically active and well-localized  $f$  orbitals with the metallic band of the host. As the Kondo screening peak develops, the optical conductivity develops a pronounced low-frequency Drude peak. Interband transitions across the Fermi surface can also yield strongly temperature-dependent features in the mid-infrared (IR) optical response.

Heavy fermion (HF) materials are usually modeled by the periodic Anderson model (PAM) or the single impurity Anderson model (SIAM). While the SIAM is able to capture the general physics of moment formation and subsequent Kondo screening and is thus sufficient to understand most of the thermodynamics of HF materials, lattice effects like coherence, and correlations between different sites are of course completely neglected in such a simplified picture. Coherence effects lead for example to a vanishing low-temperature resistivity in the metallic regime and to the formation of a band insulator in the symmetric PAM. Correlations between the sites on the other hand are responsible for various types of phase transitions, which lead to an extremely rich phase diagram with metallic, insulating or near insulating regimes depending upon the filling and model parameters.

In the metallic regime of the PAM, perhaps the most important but also controversial lattice effect is the so called exhaustion as proposed by Nozières. The “exhaustion”

problem<sup>2,3</sup> occurs when a few mobile electrons,  $n_{scr}$ , have to screen many local moments,  $n_f$ , in a metallic environment, i.e.,  $n_{scr} \ll n_f$ . This situation is engendered by the fact that only the electrons within  $T_K$  (where  $T_K$  is the single-impurity Kondo temperature) of the Fermi surface can effectively participate in screening the local moments. Thus, the number of screening electrons can be estimated as  $n_{scr} = N_d(0)T_K$ , where  $N_d(0)$  is the conduction-band density of states at the Fermi level. A measure of exhaustion is the dimensionless ratio  $p = n_f/n_{scr} = n_f/N_d(0)T_K$ .<sup>2</sup> Nozières has argued that  $p$  is roughly the number of scattering events between a local moment and a mobile electron necessary for the mobile electron’s spin to precess around a local moment by  $2\pi$ .<sup>3</sup> In the case  $p \gg 1$ , when the number of screening electrons is much smaller than the number of local moments to screen, magnetic screening is necessarily collective and the single impurity picture becomes invalid.

One further consequence of Nozières’ idea then is<sup>2</sup> that the small fraction  $n_{scr}$  of screened states may be viewed as relatively stable polaronlike particles at low temperatures  $T < T_K$ . He, thus, proposed that the screened and unscreened sites may be mapped onto particles and holes of an effective single-band Hubbard model, respectively. The screening clouds can hop from site to site and may effectively screen all the moments in a dynamical fashion.

In previous work, we extended<sup>4</sup> this argument to explain the strong reduction of the Kondo scale<sup>5</sup> in the metallic regime of the PAM. The hopping constant of Nozières’ effective model is suppressed relative to the bare one by the overlap of the screened and unscreened states. This, together with the fact that the filling of the effective Hubbard model is very close to half filling ( $n_{eff} \approx n_f - n_{scr} \approx 1$  for  $n_f = 1$ ), suggests that the relevant low-energy scale  $T_0$  of the effective model becomes very small, compared to the Kondo impurity temperature  $T_K$ .

In the crossover regime characterized by temperatures be-

tween  $T_K$ , where conventional Kondo screening begins, and the lattice scale  $T_0$ , where coherence forms, the quasiparticle peak and the screened local moment evolve much more slowly than their counterparts in the SIAM.<sup>4</sup> This provides a possible explanation for the slow evolution of the quasiparticle peak seen in photoemission experiments.<sup>6</sup> However, these results remain controversial<sup>7</sup> and are complicated by the fact that photoemission is very surface sensitive,<sup>8</sup> and probes only the first  $\approx 10 \text{ \AA}$  of the surface under investigation. Thus, predictions for less surface sensitive probes such as transport and optical conductivity are important.

In this paper, we study the effect of screening on the optical conductivity and resistivity of the PAM. We find that the resistivity is characterized by an impuritylike regime at high temperatures  $T \approx T_K$ , a crossover regime with nonuniversal behavior, and a low-temperature regime  $T \leq T_0$  where coherence begins to form. The crossover regime is the most interesting and is characterized by the exhaustion of screening states near the Fermi surface, as measured by the development of a dip centered at the Fermi energy,  $\omega=0$ , in the effective  $f$ - $d$  hybridization  $\Gamma(\omega)$ . The peak in the resistivity, which marks the upper end of the crossover regime, is a nonuniversal feature centered at a temperature  $T_e$ ,  $T_0 < T_e < T_K$ .  $T_e$  is the temperature at which exhaustion first becomes apparent as a reduction in  $\Gamma(0)$ . In the exhaustion region, the Drude weight increases strongly with temperature, and the lost weight at low  $T$  is largely transferred to a midinfrared (MIR) peak. This feature is due to interband transitions and its position matches with the minimum of the direct energy gap between the two quasiparticle bands below and above the Fermi energy. Both the Drude and MIR peaks persist up to unusually high temperatures  $T \approx 10T_0$ . We interpret the persistence of these features as well as the unusual decline of the Drude weight as  $T \rightarrow 0$  as manifestations of Nozières exhaustion scenario.<sup>9</sup>

## II. FORMALISM

The Hamiltonian of the PAM on a  $D$ -dimensional hypercubic lattice is

$$\begin{aligned}
 H = & \frac{-t^*}{2\sqrt{D}} \sum_{\langle ij \rangle \sigma} (d_{i\sigma}^\dagger d_{j\sigma} + \text{H.c.}) \\
 & + \sum_{i\sigma} (\epsilon_d d_{i\sigma}^\dagger d_{i\sigma} + \epsilon_f f_{i\sigma}^\dagger f_{i\sigma}) + V \sum_{i\sigma} (d_{i\sigma}^\dagger f_{i\sigma} + \text{H.c.}) \\
 & + \sum_i U (n_{fi\uparrow} - 1/2)(n_{fi\downarrow} - 1/2). \quad (1)
 \end{aligned}$$

In Eq. (1),  $d(f)_{i\sigma}^{(\dagger)}$  destroys (creates) a  $d(f)$  electron with spin  $\sigma$  on site  $i$ . The hopping is restricted to the nearest neighbors and scaled as  $t=t^*/2\sqrt{D}$ . We take  $t^*=1$  as our unit of energy.  $U$  is the screened on-site Coulomb repulsion for the localized  $f$  states and  $V$  is the hybridization between  $d$  and  $f$  states. This model retains the features of the impurity problem, including moment formation and screening, but is further complicated by the lattice effects.

Metzner and Vollhardt<sup>10</sup> observed that the irreducible selfenergy and vertex functions become purely local as the coordination number of the lattice increases. As a conse-

quence, the solution of an interacting lattice model in  $D = \infty$  may be mapped onto the solution of a local correlated impurity coupled to a self-consistently determined host.<sup>11</sup> We employ the quantum Monte Carlo (QMC) algorithm of Hirsch and Fye<sup>12</sup> to solve the remaining impurity problem and calculate the imaginary time local Green's functions. We then use the maximum entropy method<sup>13</sup> (MEM) to find the  $f$  and  $d$  density of states and the selfenergy.<sup>14</sup> In the limit of  $D = \infty$  the two-particle vertex corrections to the optical conductivity  $[\sigma(\omega)]$  vanish identically due to symmetry restrictions.<sup>15</sup> Hence,  $\sigma(\omega)$  can be calculated by the knowledge of one-particle selfenergy through a particle-hole bubble diagram which includes the appropriate electron-photon interaction vertices  $e\mathbf{v}_k$  at each end. A straightforward calculation of this diagram leads to,<sup>16</sup>

$$\begin{aligned}
 \sigma_{xx}(\omega) = & \frac{e^2 \pi}{\mathcal{V}D} \int_{-\infty}^{+\infty} d\epsilon \frac{f(\omega) - f(\epsilon + \omega)}{\omega} \\
 & \times \int_{-\infty}^{+\infty} dy \rho(y) A_d(y, \epsilon) A_d(y, \epsilon + \omega), \quad (2)
 \end{aligned}$$

where  $\mathcal{V}$  is the lattice volume,  $f$  is the Fermi function,  $A_d(\epsilon_k, \omega) = -1/\pi \text{Im}[G_d(k, \omega)]$  is the conduction-band spectral function and  $\rho(y) = \exp(-y^2)/\sqrt{\pi}$  is the noninteracting density of states.

## III. RESULTS

We calculated the transport for a variety of model parameters. The QMC-MEM results are limited to relatively small values of  $U/V$  by the QMC procedure and relatively low temperatures where MEM may be used to calculate the dynamics. Here, we present QMC results for  $U=1.5$ ,  $V=0.6$ ,  $n_f \approx 1$  for three conduction-band fillings  $n_d=0.4, 0.6$ , and  $0.8$ . The impurity scale  $T_K$  was calculated by extrapolating the local susceptibility to  $T=0$  [i.e.,  $T_K=1/\chi_{imp}(T \rightarrow 0)$ ]. The lattice Kondo temperature was similarly calculated by extrapolating the *effective* local susceptibility of the PAM, which is the additional local susceptibility due to the introduction of the effective impurity into a host of  $d$ -electrons.<sup>14</sup> These extrapolations result  $T_K=0.2, 0.46, 0.5$  and  $T_0=0.017, 0.055, 0.149$  for the three band fillings mentioned above, respectively.

### A. Optical Conductivity

The real part of the optical conductivity calculated with QMC-MEM is plotted versus frequency in Fig. 1 for several temperatures. As the temperature is lowered  $T \leq T_K$  two features begin to develop, a Drude peak at zero frequency, associated with free quasiparticles, and a mid-IR peak at  $\omega \approx 1$  generally associated with an interband transition as we will discuss later.

To be consistent with the way that experimental data is usually analyzed the features in  $\sigma(\omega)$  are fit to a Lorentzian plus two (asymmetric) harmonic-oscillator forms for the higher-energy peak

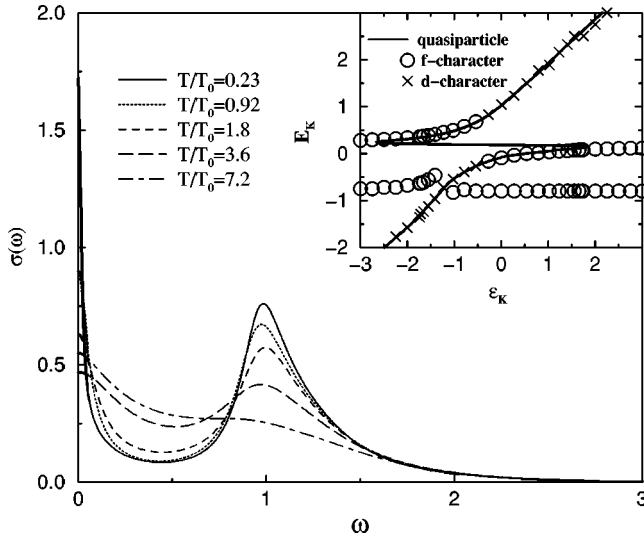


FIG. 1. Optical conductivity for various temperatures when  $U = 1.5$ ,  $V = 0.6$ ,  $n_f \approx 1$ ,  $n_d = 0.6$ , and  $T_0 = 0.055$ . Both Drude and mid-IR peaks are present and persist up  $T/T_0 \geq 10$ . The inset shows the corresponding band energies  $E_k$  plotted vs the bare d-band dispersion  $\epsilon_k$  when  $T/T_0 = 0.46$ . The solid line shows the quasiparticle energy calculated as the real part of the Green's functions poles. The symbols show the positions of the maxima in the  $f$  and  $d$  spectral functions. The mid-IR peak in the optical conductivity is due to direct transitions between occupied and unoccupied quasiparticle states.

$$\sigma(\omega) \approx \frac{D_0}{\pi} \frac{\tau}{1 + \omega^2 \tau^2} + \frac{C_{MIR}}{\pi} \frac{\omega^2 \Gamma_{MIR}}{\omega^2 \Gamma_{MIR}^2 + (\omega^2 - \omega_{MIR}^2)^2} + \frac{C_{inc}}{\pi} \frac{\omega^2 \Gamma_{inc}}{\omega^2 \Gamma_{inc}^2 + (\omega^2 - \omega_{inc}^2)^2}, \quad (3)$$

with  $\tau$  the relaxation time of the “free” quasiparticles, and the constants  $C_{MIR}$ ,  $\omega_{MIR}$ , and  $\Gamma_{MIR}$  are respectively the weight, center, and width of the mid-IR peak. As shown in Fig. 2(a), in order to improve the fitting procedure we include a second harmonic-oscillator form centered at  $\omega_{inc} \approx 0.1$ . Since this weight cannot be fit to the Drude form, part of the low-frequency spectral weight remains incoherent as  $T$  is lowered. An alternative method to separate the contributions of the Drude and the mid-IR peak to the spectral weight is to fit the optical conductivity data to a “generalized” Drude form and a harmonic-oscillator with strength  $C_{MIR}^*$  for the mid-IR region as discussed above

$$\sigma(\omega) \approx \frac{D^*}{\pi} \frac{\tau}{1 + (\omega\tau)^\alpha} + \frac{C_{MIR}^*}{\pi} \frac{\omega^2 \Gamma_{MIR}^*}{\omega^2 \Gamma_{MIR}^{*2} + (\omega^2 - \omega_{MIR}^{*2})^2}. \quad (4)$$

For a generic Fermi-liquid model  $\alpha = 2$  as was assumed in the previous fitting form. But, it turns out that treating  $\alpha$  as a fitting parameter renders the use of incoherent harmonic-oscillator unnecessary as shown in Fig. 2. The inset to this figure shows the value of exponent  $\alpha$  as a function of  $T$ .

The spectral weights  $D_0$ ,  $C_{MIR}$ ,  $C_{inc}$ , as well as those from the “generalized” fit  $D^*$  and  $C_{MIR}^*$  are plotted in Fig. 3 when  $U = 1.5$ ,  $V = 0.6$ ,  $n_f \approx 1$  and  $n_d = 0.6$  ( $T_0 = 0.055$ ).

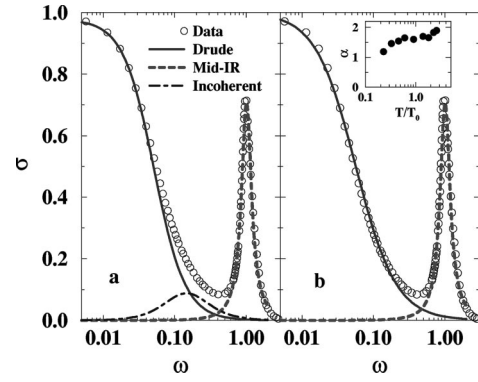


FIG. 2. Two fitting schemes for separating the share of Drude and interband transition to the optical conductivity. The model parameters are the same as in the previous figure and  $T/T_0 = 0.46$ . (a) Fitting to Eq. 3, a Fermi-liquid Drude form and two harmonic-oscillator forms. One of the harmonic-oscillators accounts for the interband transitions in the mid-IR region and the other for the low frequency spectral weight that remains incoherent. (b) Fitting to Eq. 4, a “generalized” Drude form for the low frequency part and a harmonic-oscillator for the mid-IR region. Using the exponent in the “generalized” Drude form as a fitting parameter (shown in the inset) renders the use of an incoherent harmonic-oscillator peak unnecessary.

The most surprising result is that there is a significant transfer of weight from high to low frequencies with increasing temperature. The weight in the Drude peak, as measured by either  $D_0$  or  $D^*$ , rises with temperature at low  $T$ . This feature was independent of the fitting procedure applied and was even found if the extrapolation technique of Scalapino *et al.*<sup>17</sup> was employed at low temperatures  $T < T_K$ . The opposite trend is generally expected since the Drude peak is associated with the buildup of quasiparticle weight in the single-particle spectra at low temperatures.

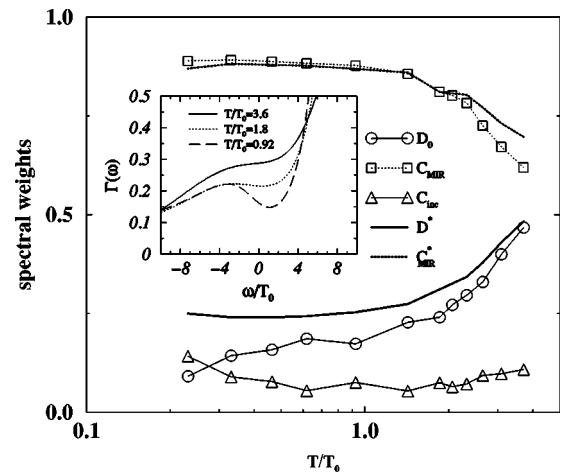


FIG. 3. The Drude, mid-IR and incoherent weights vs temperature when  $U = 1.5$ ,  $V = 0.6$ ,  $n_f \approx 1$ ,  $n_d \approx 0.6$ , and  $T_0 = 0.055$ . The coefficients  $D_0$ ,  $C_{MIR}$ , and  $C_{inc}$  ( $D^*$  and  $C_{MIR}^*$ ) were determined from a fit to Eq. (3) [Eq. (4)]. The inset shows the effective  $f$ - $d$  hybridization  $\Gamma(\omega) = \text{Im}[1/G_f(\omega) + \Sigma(\omega)]$  plotted vs  $\omega$  for several different temperatures. The weight in the Drude peak falls with  $\Gamma(0)$  since the weight in the quasiparticle peak is expected to vary as  $\sim \exp[-\pi U/8\Gamma(0)]/\Gamma(0)$  (see text).

To interpret the drop in the Drude weight with lowering  $T$ , we calculate the effective hybridization strength  $\Gamma(\omega)$ ,

$$\Gamma(\omega) = \text{Im} \left( \Sigma(\omega) + \frac{1}{G_f(\omega)} \right), \quad (5)$$

where  $G_f(\omega)$  is the local  $f$  Green's function and  $\Sigma(\omega)$  is the local  $f$ -electron selfenergy.  $\Gamma(\omega)$  is a measure of the hybridization between the effective impurity in the DMF problem and its medium [for example, in the SIAM  $\Gamma(\omega) = \pi V^2 N_d(\omega)$ , where  $N_d(\omega)$  is the  $d$ -band density of states]. The inset to Fig. 3 shows the effective hybridization for the PAM near the Fermi energy.  $\Gamma(\omega)$  begins to develop a dip at the Fermi energy at roughly the same temperature where Drude weight begins to drop.

The formation of this dip in  $\Gamma(\omega)$  can be interpreted as an effective reduction or ‘‘exhaustion’’ of the states near the Fermi energy responsible for screening the local moments. In infinite dimensions, other mechanisms which could be responsible for the dip, such as non-local spin or charge correlations, are absent<sup>18</sup>. We therefore believe that it can be taken as direct evidence for Nozières' exhaustion scenario. Concomitant with the development of this dip is a drop in the quasiparticle weight as may be seen from the following simple qualitative argument: The relevant low-energy scale is expected to vary roughly like the Kondo temperature of the effective impurity model with  $\Gamma(\omega)$  as medium, i.e.,  $T_0 \sim \exp[-\pi U/8\Gamma(0)]$ . Since this scale also sets the width of the quasiparticle peak, whose height is on the other hand fixed to  $1/\pi\Gamma(0)$  by Friedel's sum rule, the weight in the quasi-particle peak is proportional to  $\exp[-\pi U/8\Gamma(0)]\Gamma(0)$ , which falls exponentially with decreasing  $\Gamma(0)$ . Since the Drude peak is formed from quasiparticle excitations, the fall in the  $\Gamma(0)$  also corresponds to a loss in Drude weight.

The weight lost in the Drude peak as  $T$  decreases is gained by both the mid-IR peak and the low-frequency incoherent part since we find the total spectral weight to be roughly constant in  $T$ . The weight gained in the incoherent part is reflected by an increase in  $C_{inc}$  and by the reduction of the exponent  $\alpha$ . We observe that for  $T \lesssim T_0$  the exponent starts to deviate from its Fermi-liquid value 2, indicating that additional weight is building up in the tail of the low-frequency peak. The temperature dependence of  $D^*$  is basically the same as that of  $D_0 + C_{inc}$  (cf. Fig. 3) suggesting that there is a low-frequency incoherent contribution to the spectral spectral function, in addition to the quasiparticle peak, due to non-Fermi-liquid nature of the problem in this parameter regime. The remaining transferred weight is gained by the peak in the mid-IR region, which is due to excitations between the occupied and unoccupied bands states. Since the optical conductivity is constructed from a convolution of lattice spectral functions, the origin of this peak can be confirmed by inspecting the dispersion of these bands, which is plotted in the inset to Fig. 1. Here, the solid line is determined from the real part of the poles of the lattice propagators, thus it represents the quasiparticle dispersion. The location of the peaks in the single-particle spectra are denoted by the symbols. The singly occupied  $f$  level appears as an almost dispersionless band below the Fermi energy. The energy of the mid-IR peak coincides with that of the interband transition between the two quasiparticle bands below and

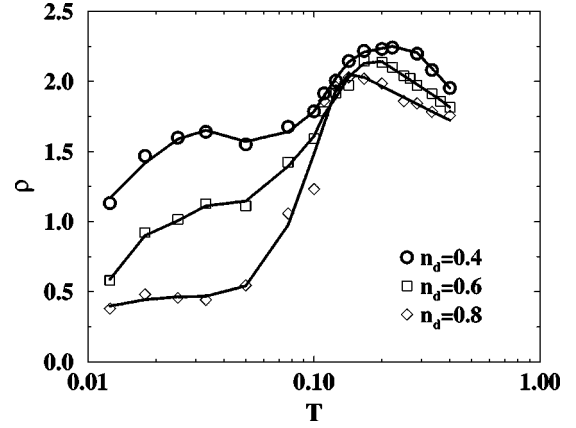


FIG. 4. The resistivity vs temperature calculated with QMC-MEM when  $U = 1.5$ ,  $V = 0.6$ ,  $n_f \approx 1$  for  $n_d = 0.4$ ,  $0.6$  and  $0.8$  (with  $T_0 = 0.017$ ,  $0.055$ , and  $0.149$ , respectively). The solid lines are from fits to a polynomial. At high temperatures, the resistivity has an impurity-like log-linear regime which terminates maximum at  $T = T_e$ .  $T_e$  is nonuniversal in that it is independent of  $T_K$  or  $T_0$  which increase with  $n_d$ ; whereas  $T_e$  decreases with  $n_d$ . When  $n_d = 0.4$  and  $0.6$ ,  $T_e$  corresponds to the temperature at which exhaustion becomes apparent as a dip in  $\Gamma(\omega)$ . For  $T < T_e$ , the resistivity shows a nonuniversal crossover region (see text). When  $n_d = 0.4$  and  $0.6$ , at still lower temperatures the resistivity begins to drop quickly at  $T \approx T_0$ , indicating the onset of Fermi-liquid formation and coherence. However for  $n_d = 0.8$  there is no such drop consistent with the proximity to the insulating regime ( $n_f = n_d = 1$ ).

above the Fermi energy at  $\epsilon_k \approx 0$  (this value of  $\epsilon_k$  is special since it represents most of the points in the Brillouin zone of the infinite dimensional lattice.)

Both the Drude peak and the mid-IR peak in  $\sigma(\omega)$  persist up to unusually high temperatures  $T \approx 10T_0$ . In the conventional Kondo picture, based upon the single-impurity model, the quasiparticle peak in the density of states, and hence both of these features in  $\sigma(\omega)$ , are expected to disappear at much lower temperatures relative to the Kondo scale. The slow evolution of these features may be due to a crossover between two energy scales;<sup>5,4</sup>  $T_K$ , the screening scale of the impurity model with the same parameters as the PAM, which is the temperature where screening starts, and  $T_0$  the Wilson-Kondo scale of the lattice. This screening regime is extended, over that in the SIAM, because of the reduction in  $\Gamma(0)$ , i.e., as  $T$  is lowered below  $T_K$ , the Kondo scale of effective impurity problem in the DMFA is self-consistently reduced. Thus, the slow evolution of  $D_0$ ,  $C_{MIR}$  and the quasiparticle peak itself are direct consequences of exhaustion.

## B. Resistivity

The resistivity  $\rho = 1/\lim_{\omega \rightarrow 0} \sigma(\omega)$  also displays anomalies due to exhaustion.  $\rho$  versus  $T$  from a QMC-MEM calculation is shown in Fig. 4 in a semilog plot for three different conduction band fillings  $n_d$ .

We can see the interplay between the different energy scales of the PAM in Fig. 4 and distinguish three distinct characteristic temperature regions for the resistivity. (i) A region of log-linear resistivity, which occurs at high temperatures  $T \gtrsim T_K$  where the single impurity physics is dominant and the correlated sites act like independent (incoherent)

scattering centers. As a result, the resistivity displays the log-linear behavior of a dilute magnetic alloy. (ii) As the temperature is lowered, the resistivity reaches a maximum value at  $T=T_e$ . Note that  $T_e$  is nonuniversal in that it is independent of  $T_K$  or  $T_0$ , which increase with  $n_d$ ; whereas  $T_e$  decreases with  $n_d$ . At least for the  $n_d=0.4$  and 0.6 datasets,  $T_e$  corresponds to the temperature at which exhaustion first becomes apparent as a dip in  $\Gamma(\omega)$ . As the temperature is lowered further,  $T<T_e$ , a pronounced dip begins to develop in  $\Gamma(\omega)$ , and is accompanied by a rapid drop in the resistivity. Then, as the decline in  $\Gamma(0)$  slows, the resistivity falls more slowly. Since the impurity scattering rate is expected to vary like  $\sim \ln\{T/\sqrt{\Gamma(0)U}\exp[-8U/\pi\Gamma(0)]\}$ ,<sup>19</sup> the resistivity can fall with decreasing  $\Gamma(0)$  even though the system has not begun to form a Fermi liquid. Partial Fermi-liquid formation can also contribute to the drop; however, this effect would be suppressed for small  $n_d$  by exhaustion and the concurrent reduction of the effective Kondo scale. For  $n_d\approx 0.6$  it is uncertain which of the two mechanisms has the dominant contribution to the drop in the resistivity at the top of the crossover regime. Also it is unclear why the crossover regime becomes less pronounced as  $n_d$  decreases. However, it seems likely that the drop for small  $n_d$ , where exhaustion is most pronounced, is due the drop in the scattering rate. Whereas for  $n_d\rightarrow 1$ , where there is no exhaustion [the Kondo scale  $T_0$  is actually enhanced relative to the impurity scale  $T_K$  (Refs. 9 and 14)] it seems likely that the initial drop is due to partial Fermi-liquid formation. (iii) Finally, as the temperature is reduced further, for conduction band fillings  $n_d=0.4$  and 0.6, the resistivity begins to drop quickly at  $T\approx T_0$ , indicating the onset of Fermi-liquid formation at  $T_0$  for these fillings. However for  $n_d=0.8$  there is no indication of this for temperatures well below  $T_0$ . When  $n_f=n_d=1$ , the PAM forms an insulating gap of width  $\approx T_0$ <sup>14</sup> (which is resonantly enhanced over the impurity scale  $T_K$ ). Thus, for  $n_d\leq 1$ , we expect a drop in the resistivity to occur when the temperature equals roughly the energy difference between the chemical potential and the bottom of the gap.

#### IV. COMPARISON WITH EXPERIMENT

Exhaustion should be most prevalent in heavy fermion materials with low-carrier concentration or a low density of conduction band states at the Fermi surface. One such material, for which an extensive study of the optical conductivity has been done, is  $\text{Yb}_4\text{As}_3$  with a Kondo scale of  $T_0\approx 40$  K.<sup>20</sup> This material has strongly temperature-dependent Drude and MIR (at roughly 0.4 eV) peaks for temperatures ranging from 39 to 320 K, as predicted by our

model calculation. In addition, there is a very significant weight transfer from the Drude peak to the MIR peak as the temperature increases over this range.<sup>21</sup> There is also some evidence for a Drude weight which drops with lowering the temperature below  $T_e$  in a typical paramagnetic HF material like  $\text{CeAl}_3$ .<sup>22</sup> Here, the transfer of weight is far less apparent, but may be inferred from the analysis of the data, where the inverse of the Drude weight (measured by fitting the optical conductivity to a Drude form at low frequencies) shows an increase with lowering  $T$  at  $\omega=0$ . However, in this material, the Drude weight vanishes quickly as the temperature is increased to  $T=10\text{K}\approx 3T_0$ . Thus, exhaustion, and the concomitant protracted evolution of  $D(T)$  would seem to be less evident in this material than it is in the low carrier system  $\text{Yb}_4\text{As}_3$ . Unfortunately, there is not enough optical data available for paramagnetic HF systems to determine whether the drop in the Drude weight and other features associated with exhaustion are generic features or even to determine their dependence on the f-level degeneracy and the conduction band filling. We believe that a systematic study of the optical properties of low carrier density HF systems could shed significant light on the importance of exhaustion in these materials.

#### V. CONCLUSION

We have performed a QMC-MEM simulation of the infinite-dimensional periodic Anderson model to study the optical conductivity in the metallic regime. We see several anomalies, including: (i) a Drude peak which persist up to anomalously high temperatures  $T\leq 10T_0$ , (ii) a MIR peak due to interband transitions across the Fermi energy, which also persists up to high temperatures  $T\leq 10T_0$ , (iii) a significant loss of Drude weight and  $f$ - $d$  hybridization as  $T\rightarrow 0$ . We interpreted these results in terms of Nozières' exhaustion picture. Finally, we note that since optical measurements are far less surface sensitive than photoemission measurements, the presence of these features in experimental spectra could serve as less controversial evidence for exhaustion in heavy Fermion systems.

#### ACKNOWLEDGMENTS

We would like to acknowledge useful conversations with J.W. Allen, A. Arko, L. Degiorgi, M. Hettler, J. Joyce, H.R. Krishnamurthy, and G. Thomas. This work was supported by the National Science Foundation Grants Nos. DMR-9704021 and DMR-9357199, and the Ohio Supercomputing Center. J.K.F. was supported by the Office of Naval Research Grant No. YIP N000149610828.

<sup>1</sup>For a review see D. W. Hess, P. S. Riseborough, and J. L. Smith, in *Encyclopedia of Applied Physics*, edited by G. L. Trigg (VCH, New York, 1991), Vol. 7, p. 435; N. Grewe and F. Steglich, in *Handbook on the Physics and Chemistry of Rare Earths*, edited by K. A. Gschneidner, Jr. and L. L. Eyring (Elsevier, Amsterdam, 1991), Vol. 14, p. 343.

<sup>2</sup>P. Nozières, *Ann. Phys. (Paris)* **10**, 19 (1985).

<sup>3</sup>P. Nozières, *Eur. Phys. J. B* **6**, 447 (1998).

<sup>4</sup>A. N. Tahvildar-Zadeh, M. Jarrell, and J. K. Freericks, *Phys. Rev. Lett.* **80**, 5168 (1998).

<sup>5</sup>A. N. Tahvildar-Zadeh, M. Jarrell, and J. K. Freericks, *Phys. Rev. B* **55**, R3332 (1997).

<sup>6</sup>J. M. Lawrence *et al.*, *J. Magn. Magn. Mater.* **108**, 215 (1992); J. Joyce *et al.*, *Physica B* **186-188**, 31 (1993); R. I. R. Blyth *et al.*, *Phys. Rev. B* **48**, 9497 (1993); J. J. Joyce *et al.*, *Physica B* **205**, 365 (1995).

- <sup>7</sup>For example, see J. J. Joyce *et al.*, Phys. Rev. Lett. **68**, 236 (1992); **72**, 1774 (1994); L. H. Tjeng *et al.*, *ibid.* **72**, 1775 (1994).
- <sup>8</sup>F. Reinert *et al.*, Phys. Rev. B **58**, 12 808 (1998).
- <sup>9</sup>T. M. Rice and K. Ueda, Phys. Rev. B **34**, 6420 (1986).
- <sup>10</sup>W. Metzner and D. Vollhardt, Phys. Rev. Lett. **62**, 324 (1989); see also E. Müller-Hartmann, Z. Phys. B **74**, 507 (1989).
- <sup>11</sup>Th. Pruschke, M. Jarrell, and J. K. Freericks, Adv. Phys. **42**, 187 (1995); A. Georges, G. Kotliar, W. Krauth, and M. Rozenberg, Rev. Mod. Phys. **68**, 13 (1996).
- <sup>12</sup>J. E. Hirsch and R. M. Fye, Phys. Rev. Lett. **56**, 2521 (1989).
- <sup>13</sup>M. Jarrell and J. E. Gubernatis, Phys. Rep. **269**, 133 (1996).
- <sup>14</sup>M. Jarrell, Phys. Rev. B **51**, 7429 (1995).
- <sup>15</sup>A. Khurana, Phys. Rev. Lett. **64**, 1990 (1990).
- <sup>16</sup>H. Schweitzer and G. Czycholl, Phys. Rev. Lett. **67**, 3724 (1991).
- <sup>17</sup>D. J. Scalapino, S. White, and S. Zhang, Phys. Rev. B **47**, 7995 (1993).
- <sup>18</sup>A recent iterated perturbation study of the PAM confirms the exhaustive nature of the dip in effective hybridization at the Fermi energy, N. S. Vidhyadhiraja, A. N. Tahvildar-Zadeh, M. Jarrell, and H. R. Krishnamurthy (unpublished). Also, a  $T=0$  NRG study shows the development of this dip as the conduction-band filling is decreased and the system goes into the exhaustion regime, Th. Pruschke, R. Bulla, M. Jarrell, and A. N. Tahvildar-Zadeh (unpublished).
- <sup>19</sup>This is the scattering rate for the Kondo impurity problem with the Kondo exchange coupling approximated by  $J \approx 8V^2/U$ . See, for example, A. C. Hewson, *The Kondo Problem to Heavy Fermions* (Cambridge University Press, NY, 1993).
- <sup>20</sup>S. Kimura, A. Ochiai, and T. Suzuki, Physica B **230-232**, 705 (1997).
- <sup>21</sup>A quasi-one-dimensional model with strong spin fluctuations has also been proposed as an explanation for the observed low-temperature anomalies in this material. See P. Fulde, Physica B **230-232**, 1 (1997).
- <sup>22</sup>A. M. Awasthi, L. Degiorgi, and G. Gruner, Phys. Rev. B **48**, 10 692 (1993).